7th CCM International Conference on Pressure and Vacuum Metrology
7th International Conference IMEKO TC16
Washington DC, USA, May 15-19, 2023

Recent research results on piston gauges

W. Sabuga[1]

[1] *Physikalisch-Technische Bundesanstalt (PTB), Braunschweig, Germany, wladimir.sabuga@ptb.de*

***Abstract* – Since the end of 20th century, a big progress has been achieved in the pressure metrology based on piston gauges. It includes a significant reduction of measurement uncertainty, an extension of the measurement range to lower pressures for piston gauges used as primary pressure standards and new measurement techniques for different pressure types. The paper gives a review of this progress with presenting main new approaches applied and results achieved.**

I. INTRODUCTION

New demands on accurate pressure measurements, arisen in the last two decades, evoked development of new pressure balances and advanced methods for their characterization. Redetermination of the Boltzmann constant (k_B) by the Dielectric Constant Gas Thermometry (DCGT), which required absolute pressure of helium gas to be measured up to 7 MPa with an accuracy of 1 ppm [1], [2], has stimulated development of new state-of-the-art pressure balances. With new commercially available force-compensated piston gauges [3], [4], it became possible to measure absolute and gauge pressures down to 1 Pa, which raised the question about traceability of these novel piston gauges at low pressures. Industrial needs for accurate negative and low positive gauge pressure measurement required suitable reference standards and calibration methods, which could be established using piston gauges [5].

II. PRESSURE BALANCES AS PRIMARY STANDARDS OF ABSOLUTE PRESSURE

Pressure balances, operable in absolute pressure mode, with the effective area traceable to standards of length by dimensional measurements, serve as primary pressure standards. For the DCGT experiments on redetermination of k_B, only pressure balances appeared to have a potential to measure absolute pressure in helium with a required relative standard uncertainty of 1 ppm up to 7 MPa. Special pressure balances, further referred to as Boltzmann pressure balances, were designed and constructed in a cooperation between PTB and Fluke-DHI, whose design addressed temperature stability, mass uncertainty, zero-pressure effective area (A_0), and pressure distortion coefficient (λ) in particular [6]. The system included two pressure balance platforms (Fig. 1), three 20 cm^2 and three 2 cm^2 piston-cylinder assemblies (PCAs), two 150 kg mass sets and automated mass handlers (AMH). The design of

Fig. 1. Boltzmann pressure balances

the PCAs was optimized to reduce pressure distortion coefficients and mounting induced deformations. In order to perform automated cross-floats with the pressure balances in gauge or absolute mode, differential pressure cells were applied to indicate pressure equilibrium.

A. Primary characterization and pressure measurements in nitrogen

Between 2008 and 2011, diameters, straightness and roundness of the pistons and cylinders were repeatedly measured using different dimensional instruments [7], [8], with the lowest standard uncertainties of piston and cylinder diameters of 5 nm and 10 nm, respectively. With this data, radii of generatrix and circle traces were generated using as a criterion a minimum sum of squired discrepancies between the diametric, straightness and roundness data by applying the approach described in [9]. The standard uncertainties of the radii of the three 20 cm^2 PCAs lied between 8 and 19 nm and contributed to the relative uncertainties of A_0 by 0.5 to 0.8 ppm [10].

The effective areas were determined by the Dadson theory [11] with the pressure distribution in the piston-cylinder gap calculated by the methods of rarefied gas dynamics (RGD) taking into account real properties of the pressure-transmitting gas, nitrogen or helium [10], [12].

The pressure distortion coefficients of the PCAs were determined by iterative calculation of the elastic distortion by the finite element method and the pressure distribution by the RGD modelling, for different operation modes and gases and taking into account real dimensional properties of the PCAs [13]. The Young modulus (E) and the Poisson coefficient (μ) of the tungsten carbide hard alloy, which the PCAs are made of, were determined by the Resonant Ultrasound Spectroscopy with uncertainties $u(E)$ = 1.9 GPa and $u(\mu)$ = 0.0013 [14]. As λ were found depending on pressure, they were presented in the form

$$\lambda = \lambda_1 + \lambda_2 p \qquad (1)$$

with combined uncertainties $u(\lambda) \leq 0.10\cdot 10^{-6}$ MPa^{-1} for the 20 cm^2 and $u(\lambda) \leq 0.034\cdot 10^{-6}$ MPa^{-1} for the 2 cm^2 PCAs [10].

Between 2008 and 2011, cross-float measurements for all possible 10 pairs of three 20 cm^2 and two 2 cm^2 PCAs were carried out in absolute pressure mode with nitrogen, and some additional measurements with helium. For each cross-floated pair, typically 180 with a minimum of 72 and maximum of 327 points were taken. For the two 2 cm^2 PCAs, the cross-float results showed necessity to correct their theoretical λ by $\pm 2.8\cdot 10^{-7}$ MPa^{-1}. After this correction, such zero-pressure effective areas A_i, $i = 1,\ldots,n$, of $n = 5$ PCAs were defined which provide best agreement with the dimensional effective areas $A_{\mathrm{d}i}$ and experimental cross-float ratios R_{ij} of PCAs' effective areas of PCAs i and j, $i = 1,\ldots,n$, $i \neq j$, according to

$$\sum_i^n \left(\frac{A_{di}-A_i}{A_{di}u_{di}}\right)^2 + \sum_i^{n-1}\sum_{j=i+1}^{n}\left(\frac{R_{ij}-A_i/A_j}{R_{ij}u_{Rij}}\right)^2 \rightarrow \min, \quad (2)$$

where $u_{\mathrm{d}i}$ and u_{Rij} are relative uncertainties of $A_{\mathrm{d}i}$ and R_{ij}, respectively. Details of this effective areas' synchronization procedure are described in [15]. The relative standard uncertainties of A_i were found to be 1.1 to 1.2 ppm for the 20 cm^2 and 1.5 to 1.6 ppm for the 2 cm^2 PCAs. These uncertainties included the uncertainties of $A_{\mathrm{d}i}$, R_{ij}, and uncertainty contributions due to discrepancies between A_i and $A_{\mathrm{d}i}$, as well as A_i/A_j and R_{ij}. Fig. 2 shows the effective area of PCA 1342 determined by cross-floats against 4 PCAs after synchronization of their A_0. All measurement results lie within ±1.5 ppm with a standard deviation of 0.55 ppm.

B. Final characterization and pressure measurements in helium

Between 2011 and 2014, a second experimental characterization campaign with measurements in helium was carried out, in which three 20 cm^2 and three 2 cm^2 PCAs were compared with each other in all possible 15 combinations [16]. For each of 12 cross-float pairs of the 20 cm^2 and 2 cm^2 PCAs, 159 to 315 cross-floats were performed. For 3 pairs of the 2 cm^2 PCAs, 456 to 618 points were taken. In the second measurement campaign, further improvements were achieved as for consistency of 2 cm^2 PCAs' λ, better agreement between theoretical $A_{\mathrm{d}i}$ and experimental cross-float ratios R_{ij}, and reduction of the experimental standard deviation of the cross-float measurements by a factor of 1.1 to 1.5. At the same time,

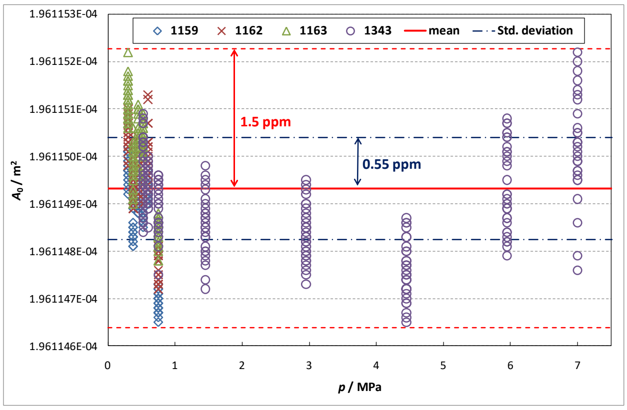

Fig. 2. Effective area of PCA 1342

all changes of R_{ij} lied between -0.76 and 1.4 ppm and agreed with their standard uncertainties. The results and their uncertainties for A_0 for nitrogen and helium are presented in Table 1.

Table 1. Effective areas and their type A, B and combined uncertainties in ppm of the Boltzmann PCAs.

PCA	2010, N_2				2014, He			
	A_0/cm^2	u_A	u_B	u	A_0/cm^2	u_A	u_B	u
1159	19.610121	0.2	1.2	1.2	19.610118	0.44	0.69	0.81
1162	19.610056	0.2	1.1	1.1	19.610052	0.30	0.63	0.69
1163	19.610429	0.4	1.1	1.2	19.610425	0.54	0.66	0.86
1341					1.9610547	0.53	0.80	0.96
1342	1.9611503	0.6	1.3	1.5	1.9611516	0.45	0.76	0.88
1343	1.9610952	0.9	1.3	1.6	1.9610957	1.42	0.78	1.62

Compared with 2010, the uncertainties of A_0 could be reduced by a factor of maximum 1.7. In addition, the results demonstrated A_0 to be invariant to gas sort, N_2 and He, within 1 ppm. PCA 1342 with the lowest $u(A_0)$ was further selected and used for pressure measurement in the DCGT experiments on k_B measurement [17]. The uncertainty budget for pressure 7 MPa with main uncertainty contributions is given in Table 2.

C. Long-term stability of effective area

In 2021, 20 cm^2 PCAs 1159 and 1163 were dimensionally re-measured. Unfortunately, the state-of-the-art comparator for diametric measurements was not accessible, so that diameters were measured using a universal dimensional instrument with a higher uncertainty than in 2010, namely with 20 nm for both, pistons and cylinders. In Fig. 3, the results of the diametric measurements in 2021 are presented by diamonds, whereas all other symbols refer to the measurements in 2010. For PCA 1159, the mean changes of diameters are equal to -59 nm for piston and +20 nm for cylinder with a resulting relative change in A_0 equal to -0.78 ppm. For PCA 1163, when comparing the results of 2010 and 2021 obtained using the same universal dimensional instrument, the mean changes of diameters are equal to -37 nm for piston and -7 nm for cylinder, which corresponds to a relative change in A_0 equal to -0.87 ppm. This shows that the affective areas of both PCAs stayed stable within their standard uncertainties over the time of 11 years.

Table 2. Sources and their contributions in ppm to uncertainty of pressure 7 MPa measured with PCA 1342 in 2010 and 2014.

Uncertainty source	2010, N_2	2014, He
Zero-pressure effective area	1.5	0.88
Pressure-distortion coefficient	1.1	0.3
Mass measurement	0.1	0.1
Gravity acceleration	0.1	0.1
Temperature measurement	0.2	0.2
Verticality of the PCA	0.1	0.1
Combined standard uncertainty	1.9	0.98

In 2020, cross-float measurements between two 20 cm^2 and two 2 cm^2 PCAs were carried out in nitrogen gas in absolute and gauge mode. The relative changes of A_0 ratios between 2010 and 2020 are collected in Table 3.

Table 3. Changes of experimental A_0 ratios from 2010 to 2020.

PCA_i/PCA_j	ΔR_{ij} / ppm	
	p_{abs}	p_e
1159/1163	0.73	0.37
1163/1342	-2.1	-0.41
1163/1343	-2.0	0.29
1342/1343	-0.76	-0.58

The measurements of 2020 were carried out with essentially lower effort than in 2010, which resulted in higher uncertainties and worse consistency. Nevertheless, the mean change of all experimental ratios R_{ij} from 2010 to 2020 is equal to only 0.5 ppm.

D. Validation of DCGT based thermodynamic pressure standard

After fixing the Boltzmann constant in 2019, DCGT experiments were continued at PTB to test its capability as a method for primary realisation of the pressure unit, using the idea described in [18]. From the ratio of capacitances measured by a capacitor filled with a gas at pressures p and 0, $C(p)$ and $C(0)$, the relative dielectric constant of gas (ε)

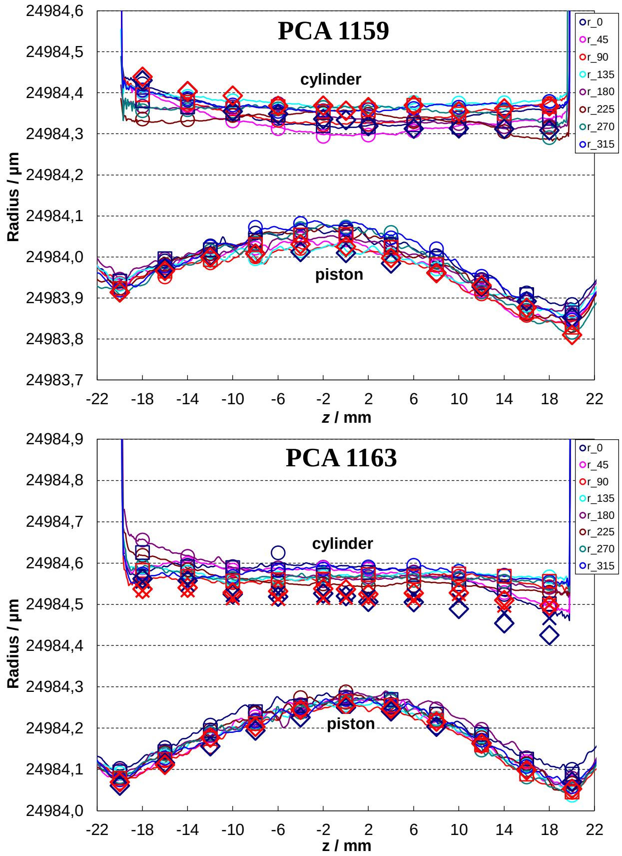

Fig. 3. Dimensional properties of PCAs 1159 and 1163 measured in 2010 (all symbols) and 2021 (diamonds)

can be determined by (3). Herewith, the gas molar density (ρ) and p can be calculated using equations (4) and (5).

$$C(p)/C(0) = \varepsilon(1+\kappa p) \quad (3)$$

$$(\varepsilon-1)/(\varepsilon+2) = A_\varepsilon \rho\,(1+b\rho+c\rho^2+d\rho^3) \quad (4)$$

$$p = k_B N_A T\,\rho(1+B\rho+C\rho^2+D\rho^3) \quad (5)$$

There, κ is capacitor's compressibility, which is calculated using capacitor material's elastic constant. A_ε is molar polarizability, b, c, d and B, C, D are dielectric and density's virial coefficients, respectively, which, for helium, can be calculated theoretically with a sufficient accuracy. Using the theoretical data as available by 2016 and their improved values obtained by 2022, thermodynamic pressures from 1 to 7 MPa in helium were realised by the DCGT method. Their calculated standard uncertainties were of 4.7 ppm and 2.8 ppm when using the theoretical data of 2016 and 2022, respectively [19], [20]. The thermodynamic pressures were compared with mechanical pressures measured by the Boltzmann pressure balance, equipped with PCA 1342, with a standard uncertainty of 1 ppm. The differences between the thermodynamic and mechanical pressures were rather irregular over the pressure range of 1 to 7 MPa with a

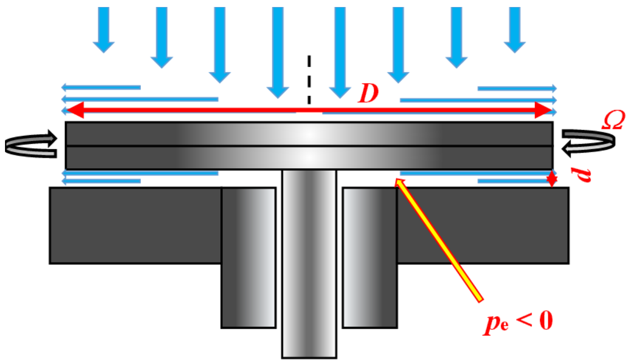

Fig. 4. Schematics of flows and loads on rotating weights

bandwidth of ±5 ppm [20].

III. GAUGE PRESSURE MEASUREMENTS AND PISTON ROTATION EFFECT

In practice, majority of pressure balance calibrations performed by national metrology institutes (NMI) and accredited laboratories are realised in gauge mode. To benefit from the progress achieved by the pressure balance metrology in the area of absolute pressure, particularly with the Boltzmann pressure balances, effects specific for operation under atmospheric conditions need to be taken into account. One of the important effects is counteraction of rotating weights with the surrounding air, which produces an additional force on the piston. This effect depends on configuration of the pressure balance and, in dependence on piston rotation rate, can affect the pressure measurement by up to $5 \cdot 10^{-4}$ relative [21], [22]. To minimize this effect, piston should be rotated with sufficiently low rates. Alternatively, a piston load correction needs to be applied [23]. In [24], the piston rotation effect was systematically studied and measured for different types of pressure balances. To better understand the nature of the piston rotation effect, a theory of an endless rotating disk was applied to analyse aerodynamic forces acting on rotating weights. According to previous ideas, centrifugally driven radial air flow at weights' upper surface induces a flow directed downwards and producing additional load and, consequently, increasing the pressure (Fig. 4). Our calculations have shown that the vertical air flow blowing onto the weights' upper surface is too week to explain experimentally observed changes of pressure. Instead, centrifugal forces acting on air in the gap between the weights and the platform cause a negative gauge pressure and, herewith, an additional, downwards directed force, which quantitively explains the piston rotation effect observed experimentally (Fig. 4). The value of this additional force (F_e) depends on rotation rate (Ω), weights diameter (D) and distance between the weights and the nearest surface (d), e.g. platform surface, see Fig. 4, and can be approximated by function (6), where d_B is thickness of the boundary layer, $f(d/d_B)$ is a numerically calculated transition function and

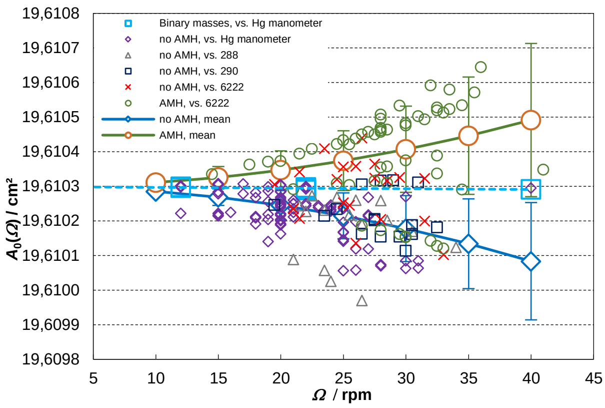

Fig. 5. Effective area of Boltzmann PCA 1159

n is power factor changing from 1 to 4 when d/d_B is changing from ∞ to 0.

$$F_e \sim \begin{cases} \Omega\, D^2, & d \gg d_B \\ \Omega^{3/2} D^4 \times [1 + D^n f(d/d_B)], & n = 1, \ldots, 4 \\ \Omega^2 D^4, & d \ll d_B \end{cases} \quad (6)$$

The theory was proved by experiments in which gaps of different d were realised by fixing a plate at different distances from rotating weights below and above them. These experiments showed equality of positive and negative additional forces when the plate was placed at the same distance below and above the weights [24]. These results are important for operation of the Boltzmann pressure balances as well as any other pressure balances equipped with AMH, in which small distances of few millimetres between rotating and fixed load disks take place. The Boltzmann pressure balance was compared in gauge mode with four different primary pressure standards, a mercury manometer and three pressure balances. Results for the effective area at 100 kPa in dependence on piston rotation rate when operating the Boltzmann pressure balance with and without AMH as well as with binary masses only are shown in Fig. 5. Operation with and without AMH produces additional upwards and downwards forces, respectively, with corresponding deviations of the effective areas. Operation with binary masses, which have much smaller diameter than the main masses, shows no rotation rate dependence of the effective area. By applying a correction based on equation (6), the standard deviation of cross-float measurements with the Boltzmann pressure balance could be reduced from 1.2 to 0.7 ppm.

IV. FORCE-COMPENSATED PISTON GAUGES AS PRIMARY PRESSURE STANDARDS

Two representatives of force-compensated piston gauges are the Furness Rosenberg standard (FRS), manufactured by Furness Controls [3], and the force-balanced piston gauge FPG8601, produced by Fluke [4]. In both standards, the force of pressure acting on the piston is measured by a load cell, which allows compensating piston weight and consequently measuring essentially lower pressures than by dead-weight pressure balances, as low as about 1 Pa. Being calibrated in terms of A_0, FRS and FPG are compared with fundamental pressure standards such as pressure balances and mercury manometers, which normally is possible at pressures above few kilopascals. This raises the question about applicability of A_0, determined at high pressures, in low pressure measurements. One of the ways to resolve this problem consists in determining their A_0 from dimensional measurements as it is done with classical pressure balances. However, when the force-compensated piston gauges are operated at low pressures in absolute mode, molecular properties of gas need to be taken into account when modelling the gas flow in their PCAs. Within European joined research project pres2vac [25], project partners NMIs, PTB (DE), CMI (CZ), RISE (SE) and INRiM (IT), characterized their FPG and FRS dimensionally, and University of Thessaly, UTH (GR), performed computation of A_0 of these piston gauges [26]. Since the flow in their PCA gaps is in a wide range of the Knudsen number, simulations were based on the Batnagar–Gross–Krook (BGK) kinetic model equation, while the typical Dadson and Computational Fluid Dynamics' (CFD) approaches were complimentary applied in the viscous regime. The differences of A_0 determined by kinetic and viscous approaches in absolute pressure operation mode were up to 15 ppm for FPG and up to 25 ppm for FRS. In gauge mode, the differences were below 3.5 ppm for FPG and negligibly small for FRS. In the uncertainty analysis for A_0, dimensional measurements were found as the main uncertainty source (1 to 8 ppm), followed by the accommodation coefficient characterizing the gas-surface interaction (0.3 to 2.4 ppm), while the effect of other flow, gas and modelling parameters, including gas humidity, was negligible (≤0.25 ppm). Independently, the PTB FPG was simulated at PTB by own BGK, Dadson and CFD approaches [27]. By using a 2D flow model in the CFD calculations, the uncertainty contribution due to PCA axial non-symmetry could be reduced from 11 to 0.14 ppm [28]. The differences between A_0 calculated by UTH and PTB were, at any pressure, below 0.14 ppm, at 15 kPa only 0.02 ppm. Furthermore, A_0 was determined experimentally by calibrating the FPG against a pressure balance in the pressure range of 2 to 15 kPa in absolute and gauge mode. The experimental results were consistent with the theoretical ones and allowed determination of a combined A_0 with a standard uncertainty of 4.3 ppm. Herewith, the standard uncertainty of absolute and gauge pressures measured with the PTB FPG was estimated as $u(p) = 10\ \text{mPa} + 6{\cdot}10^{-6}p$. This measurement capability was confirmed by comparison of the FPG with the PTB mercury manometer [29] in the pressure range 100 Pa to 15 kPa in gauge and absolute mode and with the PTB static expansion system [30] in the range of absolute pressure from 3 to 300 Pa [31].

V. CONCLUSIONS

With special design pressure balances and advanced characterization methods, the pressure scale from 20 kPa to 7.5 MPa was realized with a relative standard uncertainty of 1 ppm. Invariance of the effective area to gas sort, N_2 vs. He, and stability within 1 ppm over 10 years was demonstrated. Owing the lowest uncertainty, pressure balances provide a reliable tool for testing new alternative primary pressure standards. In gauge mode, counteraction of rotating weights with ambient air requires consideration. It allows performance similar to that in absolute mode to be achieved. Advanced dimensional and flow modelling methods allow force-balanced piston gauges to be characterized as primary pressure standards in the range of 1 Pa to 15 kPa with a standard uncertainty of 10 mPa + 6 ppm.

ACKNOWLEDGMENTS

The contribution of PTB colleagues T. Konczak, S. Ehlers, O. Ott and T. Bock, having performed pressure and vacuum measurements, T. Zandt, C. Gaiser and B. Fellmuth, having characterized Boltzmann pressure balances with helium and performed DCGT experiments, O. Jusko and H. Reimann, having performed dimensional measurements, PTB guest researchers T. Priruenrom (NIMT, Thailand), having studied Boltzmann pressure balances, and A. Hashad (NIS, Egypt), having studied FPG and FRS, as well as UTH colleagues S. Naris, N. Vasileiadis and D. Valougeorgis, having modelled FPG and FRS, is greatly acknowledged.

REFERENCES

[1] B.Fellmuth, Ch.Gaiser, J.Fischer, “Determination of the Boltzmann constant – status and prospects”, Meas. Sci. Technol., vol.17, 2006, pp.R145-R159.

[2] J.Fischer, B.Fellmuth, et al., “The Boltzmann project”, Metrologia, vol.55, 2018, pp.R1–R20

[3] C.G.Rendle, H.Rosenberg, “New absolute pressure standard in the range 1 Pa to 7 kPa”, Metrologia, vol.36, 1999, pp.613-615.

[4] P.Delajoud, M.Girard, “A force balanced piston gauge for very low gauge and absolute pressure”, in Proc. of 10th Intern. Metrology Congress, St Louis, France, 22–25 October 2001.

[5] D.Bentouati, Y.Durgut, P.Otal, M.Plimmer, D.Pražák, W.Sabuga, S.Ehlers, E.Sinir, “Calibration methods for negative gauge pressure down to −100 kPa”, Meas. Sci. Technol., vol.29, 2018, 10 pp.

[6] W.Sabuga, T.Priruenrom, R.Haines, M.Bair, “Design and evaluation of pressure balances with 10^{-6} uncertainty for the Boltzmann constant project”, PTB-Mitteilungen, vol.121, 2011, No.3, pp.256-259.

[7] O.Jusko, M.Neugebauer, H.Reimann, W.Sabuga, T.Priruenrom, “Dimensional calibration techniques for pressure balances to be used in the new determination of the Boltzmann constant”, Proc. of I CIMMEC – 1st Intern. Congress on Mechanical Metrology, October 8-10, 2008, Rio de Janeiro, Brazil, in Infosim – Informative Bulletin of the Interamerican Metrology System – OAS, August 2009, pp.14-23.

[8] O.Jusko, D.Bastam, M.Neugebauer, H.Reimann, W.Sabuga, T.Priruenrom, “Final results of the geometrical calibration of the pressure balances to be used for the new determination of the Boltzmann constant”, Key Engineering Materials, vol.437, 2010, pp.150-154.

[9] W.Sabuga, T.Priruenrom, “An approach to the evaluation of dimensional measurements on pressure-measuring piston-cylinder assemblies”, Proc. of 3rd Conf. on Pressure Measurement IMEKO TC16, Merida, Mexico, 2007, http://www.imeko.org/publications/tc16-2007/IMEKO-TC16-2007-074u.pdf

[10] W.Sabuga, “Pressure measurements in gas media up to 7.5 MPa for the Boltzmann constant redetermination”, PTB-Mitteilungen, vol.121, 2011, No.3, pp.247-255.

[11] R.S.Dadson, S.L.Lewis, G.N.Peggs, “The Pressure Balance – Theory and Practice”, HMSO, London, 1982.

[12] W.Sabuga, F.Sharipov, T.Priruenrom, “Determination of the effective area of piston-cylinder assemblies using a rarefied gas flow model”, PTB-Mitteilungen, vol.121, 2011, No.3, pp.260-262.

[13] W.Sabuga, T.Priruenrom, G.Molinar, G.Buonanno, T.Rabault, P.Wongthep, D.Pražák, “FEA calculation of pressure distortion coefficients of gas-operated pressure balances – EURAMET project 1039”, Measurement, vol.45, 2012, pp.2464-2468

[14] W.Sabuga, P.Ulbig, A.D.Salama, “Elastic constants of pressure balances' piston-cylinder assemblies measured with the resonant ultrasound spectroscopy”, Proc. of Intern. Metrology Conf. CAFMET-2010, Cairo, Egypt, 18-23 April 2010.

[15] W.Sabuga, T.Priruenrom, “An approach to synchronise effective areas of pressure balances”, MAPAN – J. of Metrology Soc. of India, vol.30, No.1, 2015, pp.7–13.

[16] T.Zandt, W.Sabuga, C.Gaiser, B.Fellmuth, “Measurement of pressures up to 7 MPa applying pressure balances for dielectric-constant gas thermometry”, Metrologia, vol.52, 2015, pp.S305–S313.

[17] C.Gaiser, B.Fellmuth, N.Haft, A.Kuhn, B.Thiele-Krivoi, T.Zandt, J.Fischer, O.Jusko, W.Sabuga, “Final determination of the Boltzmann constant by dielectric-constant gas thermometry”, Metrologia, vol.54, 2017, pp.280-289.

[18] M.R.Moldover, “Can a pressure standard be based on capacitance measurements?”, J. Res. Natl. Inst. Stand. Technol., vol.103, 1998, pp.167-175.

[19] C.Gaiser, B.Fellmuth, W.Sabuga, “Primary gas-pressure standard from electrical measurements and thermophysical ab initio calculations”, Nature Physics, vol.16, 2020, pp.177-180.

[20] C.Gaiser, B.Fellmuth, W.Sabuga, “Primary gas pressure standard passes next stress test”, Annalen der Physik (Berlin), 2022, No.534, 2200336, pp.1-6.

[21] D.B.Prowse, D.J.Hatt, “The effect of rotation on a gas-operated free-piston pressure gauge”, J. Phys. E: Sci. Instrum., vol.10, 1977, pp.450-451.

[22] C.M.Sutton, “The rotational frequency dependence of a pressure balance”, J. Phys. E: Sci. Instrum., vol.12, 1979, pp.466-468.

[23] J.W.Schmidt, Y.Cen, et al., “A primary pressure standard at 100 kPa”, Metrologia, vol.36, 1999, pp.525-529.

[24] O.Ott, W.Sabuga, T.Konczak, “Experimental study of piston rotation rate effect”, Proc. of 6th IMEKO Conf. on Pressure and Vacuum Measurement, Cavtat-Dubrovnik, Croatia, 11-13 Oct. 2022. DOI https://doi.org/10.21014/tc16-2022.021

[25] Industrial standards in the intermediate pressure-to-vacuum range, Short Name: pres2vac, Project No. 14IND06, EURAMET, https://www.euramet.org /research-innovation/search-research-projects/ details/project/industrial-standards-in-the-intermediate-pressure-to-vacuum-range.

[26] S.Naris, N.Vasileiadis, D.Valougeorgis, A.Hashad, W.Sabuga, “Computation of the effective area and associated uncertainties of non-rotating piston gauges FPG and FRS”, Metrologia, vol.56, 2019, pp.1-10

[27] A.S.Hashad, S.Ehlers, O.Jusko, W.Sabuga, “Characterization of a force-balanced piston gauge as a primary pressure standard”, Measurement, vol.131, 2019, pp.723-729.

[28] W.Sabuga, A.S.Hashad, S.Ehlers, “2D flow model for calculating effective area of piston-cylinder units”, Acta IMEKO, vol.9, No.5, 2020, pp.319-324.

[29] J.Jäger, “Use of a precision mercury manometer with capacitance sensing of the menisci”, Metrologia, vol.30, 1993/94, pp.553-558.

[30] T.Bock, H.Ahrendt, K.Jousten, “Reduction of the uncertainty of the PTB vacuum pressure scale by a new large area non-rotating piston gauge”, Metrologia, vol.46, 2009, pp.389-396.

[31] A.S.Hashad, W.Sabuga, S.Ehlers, T.Bock, “Validation of a PTB force-balanced piston gauge - primary pressure standard”, Acta IMEKO, vol.10, No.1, 2021, pp.271-276.